RASĀYAN *J. Chem.*
Vol. 18 | No. 3 |1574-1580| July-September | 2025
ISSN: 0974-1496 | e-ISSN: 0976-0083 | CODEN: RJCABP
http://www.rasayanjournal.com
http://www.rasayanjournal.co.in

HIGH-PERFORMANCE THERMOELECTRIC MATERIALS: 11% EFFICIENCY AND 5.2 W/CM² POWER DENSITY IN OPTIMALLY CHLORINE-DOPED PBTE-BASED THERMOELECTRICS

Sukendar[1], Jong-Soo Rhee[2] and Dianta Ginting[1,✉]

[1]Department of Mechanical Engineering, Faculty of Engineering, Mercubuana University, Jakarta 031019, Indonesia

[2]Department of Applied Physics and Institute of Natural Sciences, Kyung Hee University, Yongin 17104, South Korea

✉Corresponding author: dianta.ginting@mercubuana.ac.id

ABSTRACT

Thermoelectric materials facilitate the transformation of waste heat directly into electrical energy, offering significant potential for sustainable energy applications. This study investigates optimal chlorine doping in $(PbTe_{0.93-x}Se_{0.07}Cl_x)_{0.93}PbS_{0.07}$ thermoelectric materials across varying concentrations (x = 0.0005 to 0.2) to maximize energy conversion efficiency and power density. Results demonstrate that ultra-low chlorine doping (x = 0.0005) achieves optimal performance by significantly enhancing charge carrier density while maintaining favorable electrical conductivity and Seebeck coefficient balance. The composition $(PbTe_{0.93-x}Se_{0.07}Cl_x)_{0.93}PbS_{0.07}$ delivers exceptional thermoelectric performance with energy conversion efficiency exceeding 12% and power density surpassing 6 W/cm² at a 500 K temperature gradient. These findings establish precise low-level chlorine doping as a critical strategy for creating advanced thermoelectric materials applicable to industrial waste heat recovery and sustainable energy applications. The research contributes to advancing clean energy technologies by enabling more efficient utilization of otherwise wasted thermal energy, supporting global sustainability goals through improved energy conversion systems.

Keywords: Thermoelectric Materials, Chlorine Doping, PbTe-Based Compounds, Energy Conversion Efficiency, Power Density, Waste Heat Recovery, Sustainable Energy.

RASĀYAN*J. Chem.*, Vol. 18, No. 3, 2025

INTRODUCTION

Industrial waste heat represents approximately 20-50% of global energy consumption currently lost to the environment, highlighting an urgent need for efficient energy recovery technologies. This critical energy challenge has accelerated research into thermoelectric (TE) materials, which have been extensively studied in academia due to their capability to convert waste thermal energy into electrical power through voltage differences generated by temperature gradients, where temperature differences induce charge transport and generate thermal voltage.[1-2] TE technology offers substantial potential for residual heat recovery, portable electricity production, and renewable energy systems, directly supporting *SDG 7* (Affordable and Clean Energy) by efficiently utilizing otherwise wasted thermal resources. However, attaining optimal energy conversion efficiency enhancements in the thermoelectric performance index (ZT) is difficult. This metric relies on the voltage generated by a thermal condition difference through a thermal gradient, the Seebeck coefficient (S), electrical conductivity (σ) of the material, total thermal conductivity (κ_T), and absolute temperature (T). Mathematically, this relationship is expressed through the following equation[3]:

$$ZT = \frac{S^2 \sigma T}{\kappa_T} \quad (1)$$

Materials based on lead telluride (PbTe) are highly suitable for thermoelectric applications, particularly within the 300-800 K temperature range, because of their exceptional electronic and thermal properties, including a favorable band structure, low thermal conductivity, and tunable electronic characteristics.[4-5] One effective approach is chlorine doping, which enhances the n-type properties of PbTe by optimizing the carrier concentration and improving electrical conductivity.[6]

http://doi.org/10.31788/RJC.2025.1839282

Optimizing doping is essential for regulating charge carrier concentration and enhancing the power factor ($S^2\sigma$). In PbTe-based materials, chlorine doping increases electron density and electrical conductivity (σ) while maintaining a high thermoelectric voltage coefficient (S).[7] However, excessive doping can lead to increased carrier scattering and reduced thermoelectric performance. In addition to boosting electrical conductivity, reducing thermal conductivity in PbTe is crucial for achieving high ZT values. Thermal conductivity comprises two main components: lattice conduction (κ_l) and electronic conduction (κ_{el}). The lattice contribution (κ_l) can be substantially minimized by increasing phonon scattering, achieved by nano-structuring or introducing defects into the material.[8] On the other hand, a higher carrier concentration tends to increase the electronic thermal conductivity (κ_{el}), thereby creating a trade-off between electrical and thermal transport.[9-11] Recent research has introduced ZT_{eng} and PF_{eng} as practical approaches for evaluating thermoelectric materials over a wide temperature range. Unlike the conventional ZT parameter, ZT_{eng} assesses voltage, electrical conductivity, and thermal conductivity across an extended range for improved performance analysis, while PF_{eng} accurately represents energy conversion efficiency. Output power density (Pd) is a key metric for thermoelectric performance, as it measures energy efficiency transfer under optimal conditions. Chlorine-doped $(PbTe_{0.93-x}Se_{0.07}Cl_x)_{0.93}PbS_{0.07}$ materials exhibit high Pd values under significant temperature gradients, making them ideal for industrial waste heat recovery and power generation in extreme environments.[12-13] Moreover, chlorine doping enhances thermoelectric efficiency through increased electrical conductivity and optimized power factor while maintaining low thermal conductivity. However, excessive doping may increase carrier scattering, thereby reducing overall thermoelectric efficiency.[14] The main goal of this study is to investigate output power density (Pd), examine the performance index (ZT_{eng}), energy conversion efficiency (PF_{eng}), and maximum efficiency (η_{max}) to optimize doping concentration and enhance the effectiveness of thermoelectric materials in energy conversion applications.[15] $(PbTe_{0.93-x}Se_{0.07}Cl_x)_{0.93}PbS_{0.07}$ as a function of temperature materials with varying chlorine doping concentrations (x = 0.0005, 0.01, 0.1, and 0.2 by using Seebeck confiecient, Electric conductivity[11] and total thermal conductivity of reference $(PbTe_{0.93-x}Se_{0.07}Cl_x)_{0.93}PbS_{0.}07$.[11] The results indicate that the composition $PbTe_{0.8595}Cl_{0.0005}Se_{0.07}S_{0.07}$ exhibits the highest thermoelectric performance, achieving optimal ZT_{eng}, PF_{eng}, and output power density. This specific composition demonstrates an optimal balance among electrical conductivity, the Seebeck coefficient, and thermal resistance, culminating in a maximum efficiency exceeding 12% at a temperature gradient (ΔT) of 500 K. Precise doping control enhances the potential applications of PbTe-based materials.[11]

EXPERIMENTAL

Sample Synthesis

The synthesis of PbSe and PbS precursor compounds was carried out using high-purity elemental materials, specifically, lead (Pb), sulfur (S), and selenium (Se) of at least 99.999% purity. These elemental constituents were sealed in quartz ampoules or quartz tubes under a vacuum ($< 10^{-4}$ *Torr*) to prevent contamination and subsequently melted at 1150 °C for 12 hours with a heating rate of 5 °C/min. For the synthesis process, chlorine-doped specimens were prepared using the composition $(PbTe_{0.93-x}Se_{0.07}Cl_x)_{0.93}PbS_{0.07}$, where x takes the values 0.0005, 0.01, 0.1, and 0.2. The precursor powders were blended in stoichiometric ratios using high-purity (99.99%) lead (Pb), tellurium (Te), and lead (II) chloride ($PbCl_2$). These mixtures were meticulously sealed in evacuated tubes, then heated at 1100 °C and held at that specific temperature for 10 hours. The molten compositions were subsequently rapidly cooled in water to promote homogeneity. The produced ingots underwent an annealing process at 500 °C for 72 hours to relieve internal stresses and improve crystallinity. Following annealing, they were finely ground into powders and compacted through a heat-pressing sintering process at 500 °C under 40 MPa in a controlled vacuum, ensuring high density and a uniform microstructure.[11]

Characterization of Thermoelectric Performance

The evaluation regarding the Seebeck coefficient and the conductivity of electricity in the material was conducted using the four-point probe method to ensure accurate measurements and minimize contact resistance errors. The measurement of heat conductivity (κ) was ascertained through the utilization of the following equation:[11]

$$\kappa = \rho.Cp.D \quad (2)$$

Where ρ represents density, Cp represents the material's specific heat capacity, and D denotes the property of thermal diffusion coefficient. Thermal diffusivity (D) was measured using the laser flash method (*Netzsch LFA 457*). The measured density was ascertained through the application of the principle of Archimedes' principle.[16-17] To substantiate the reproducibility, minimizing experimental error and reliability of the thermo-electric properties, all measurements were conducted in triplicate. The experimental measurement uncertainties were defined as follows: ±3.3% for specific heat capacity, ± 2% for densities, ±4.7% for heat diffusivity, and ±7.4% for the thermoelectric efficiency coefficient.

RESULTS AND DISCUSSION

The fundamental thermoelectric properties of $(PbTe_{0.93-x}Se_{0.07}Cl_x)_{0.93}PbS_{0.07}$ materials were systematically characterized across different chlorine doping concentrations (x = 0.0005, 0.01, 0.1, and 0.2) over the temperature range of 300-800 K, as presented in Fig.-1. The experimental measurements revealed that the ultra-low doping concentration (x = 0.0005) consistently exhibited superior performance across all measured parameters. Specifically, this composition demonstrated the highest electrical conductivity values, maximum absolute Seebeck coefficient (reaching -237 $\mu V/K^{-1}$ at 750 K), optimal power factor (21 $\mu W/cm^{-1}K^{-2}$ at 500 K), and lowest thermal conductivity (0.84 $W/m^{-1}K^{-1}$ at 750 K).[11]

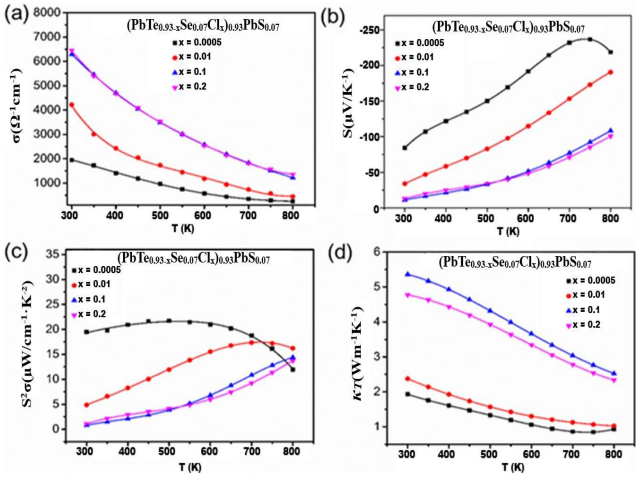

Fig.-1: The Temperature-Dependent Evolution of Thermoelectric Properties Covering (a) Electrical Conductivity, (b) Seebeck Coefficient, (c) Power Factor ($S^2\sigma$), and (d) the Overall Thermal Conductivity (κ_T) for $(PbTe_{0.93-x}Se_{0.07}Cl_x)_{0.93}PbS_{0.07}$ (x = 0.0005, 0.01, 0.1, and 0.2), as Reported in the Reference[11]

The temperature-dependent data from Fig.-1 serve as fundamental input parameters for calculating advanced engineering metrics, including ZT_{eng}, PF_{eng}, energy conversion efficiency (η), and output power density (Pd), which are analyzed in the following section. The engineering Figure of merit (ZT_{eng}), shown in Fig.-2, evaluates thermoelectric performance under practical conditions by incorporating the thermal gradient (ΔT) and represents a more realistic assessment compared to point-based ZT calculations. The significance of ZT_{eng} lies in its ability to integrate temperature-dependent material properties across the entire operating temperature range, providing accurate performance predictions for real-world thermoelectric devices. ZT_{eng} effectively accounts for practical thermoelectric performance across a temperature gradient ΔT (from hot side to cold side) by considering the continuous variation of material properties rather than single-point evaluations. The ZT_{eng} calculation is conducted through the following equation[18]:

$$ZT_{eng} = Z_{eng}T = \frac{PF_{eng}}{\Delta T \int_{T_c}^{T_h} \kappa_{(T)} dT} \quad (3)$$

Where: PF_{eng} represents the engineering power factor, κ_T represents the temperature-dependent thermal conductivity, and T_h and T_c denote the hot-side and cold-side temperatures, respectively.[18] The experimental results presented in Fig.-2, 3, 4, and 5 demonstrate that $PbTe_{0.8595}Cl_{0.0005}Se_{0.07}S_{0.07}$ achieves the highest ZT_{eng}, while excessive doping reduces performance due to increased carrier scattering, emphasizing the critical importance of precise doping control.[19]

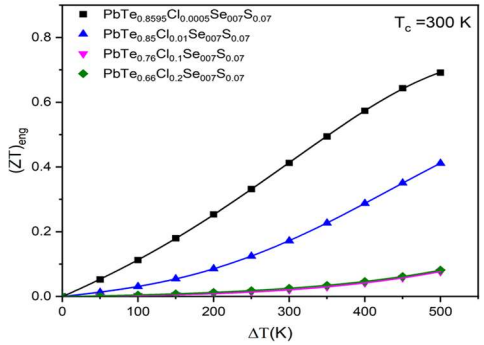

Fig-2: Temperature-Dependent Engineering Dimensionless Performance Parameter ZT_{eng} Versus Temperature Differential for T_c= 300 K In Compound Series Compounds Of $(Pbte_{0.93-X}se_{0.07}Cl_x)_{0.93}pbs_{0.07}$ (X = 0.0005, 0.01, 0.1, and 0.2)

The engineering power factor (PF_{eng}) represents a more realistic assessment of thermoelectric performance under practical operating conditions compared to conventional power factor calculations. Unlike point-based evaluations, PF_{eng} integrates temperature-dependent material properties across the entire temperature gradient, providing accurate performance predictions for real-world applications.

The calculation of PF_{eng} is conducted through the following integral[18]:

$$PF_{eng} = (\int_{T_c}^{T_h} S_{(T)}\, dT)^2 / \int_{T_c}^{T_h} \rho_{(T)} dT \quad (4)$$

Where: $S_{(T)}$ represents the temperature-dependent Seebeck coefficient, ($\mu V/K^{-1}$) obtained from experimental measurements (Fig.-1b), $\rho_{(T)}$ represents the temperature-dependent electrical resistivity ($\Omega \cdot m$), calculated as the inverse of electrical conductivity $\sigma_{(T)}$ from (Fig.-1a), T_c and T_h denote the cold-side and hot-side temperatures, respectively (with T_c = 300 K as the reference temperature), and $\Delta T = T_h - T_c$ represents the temperature gradient across the thermoelectric device. Based on the experimental data presented in Fig.-3, $PbTe_{0.8595}Cl_{0.0005}Se_{0.07}S_{0.07}$ (black squares) demonstrates significantly superior PF_{eng} performance compared to all other doping concentrations, reaching approximately 0.85 $W/m^{-1} \cdot K^{-1}$ at ΔT = 500 K. The data clearly show a non-linear relationship between temperature gradient and PF_{eng}, with performance increasing more rapidly at higher ΔT values. The experimental results demonstrate that the ultra-low doping strategy (x = 0.0005) achieves approximately 2.9 times higher PF_{eng} values compared to excessive doping (x = 0.2) at ΔT = 500 K, highlighting the critical importance of precise doping control in optimizing thermoelectric device performance for practical energy conversion applications.

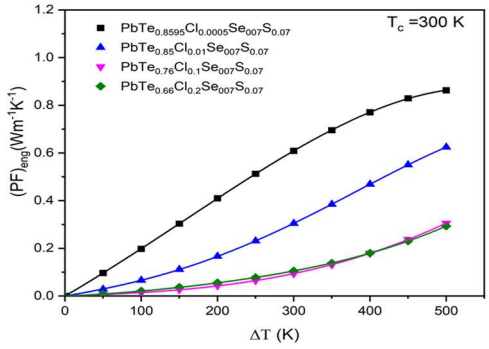

Fig.-3: Relationship between PF_{eng} (Engineering Power Factor) and the Temperature Gradient (ΔT) for $(PbTe_{0.93-x}Se_{0.07}Cl_x)_{0.93}PbS_{0.07}$ (x = 0.0005, 0.01, 0.1, and 0.2), at T_c = 300 K

The maximum thermoelectric efficiency (η_{max}) is shown in Fig.-4. The η_{max} is calculated using the following equation[18]:

$$\eta_{max} = \eta_c \frac{\sqrt{1+(ZT)_{eng}\left(\frac{\hat{\alpha}}{\eta_c}-\frac{1}{2}\right)}-1}{\hat{\alpha}\left(\sqrt{1+(ZT)_{eng}\left(\frac{\hat{\alpha}}{\eta_c}-\frac{1}{2}\right)}+1\right)-\eta_c} \quad (5)$$

Where: η_c represents the Carnot efficiency, calculated as $\eta_c = (T_h - T_c)/T_h$, $(ZT)_{eng}$ is the engineering figure of merit obtained from Fig.-2, and T_h and T_c are the hot-side and cold-side temperatures, respectively (with T_c = 300 K).

Based on the experimental data illustrated in Fig.-4, $PbTe_{0.8595}Cl_{0.0005}Se_{0.07}S_{0.07}$ (black squares) achieves the highest η_{max} of approximately 11% at ΔT = 500 K, resulting from the optimal combination of high ZT_{eng} values (0.69 from Fig.-2) and superior PF_{eng} (0.85 $W/m^{-1}\cdot K^{-1}$ from Fig.-3) in equation (5). Comparative analysis reveals a dramatic performance hierarchy: moderate doping (x = 0.01, blue triangles) achieves ~6.9% efficiency, demonstrating that the ultra-low doping strategy achieves approximately 6.8 times higher efficiency compared to excessive doping due to the simultaneous optimization of ZT_{eng} and minimization of thermal conductivity effects.[11] The output power density (Pd) represents the maximum electrical power that can be extracted per unit area from a thermoelectric device under optimal load conditions. This parameter is crucial for evaluating the practical utility of thermoelectric materials in space-constrained applications. The calculation of Pd is conducted using the following equation[18]:

$$P_d = \frac{(PF)_{eng}\Delta T}{L} \frac{m_{opt}}{(1+m_{opt})^2} \quad (6)$$

Where: $(PF)_{eng}$ represents the engineering power factor obtained from Fig.-3 ($W/m^{-1}\cdot K^{-1}$), ΔT is the temperature difference between hot and cold sides (K), mopt is the optimal load resistance ratio for maximum power transfer, and L represents the device length (m).

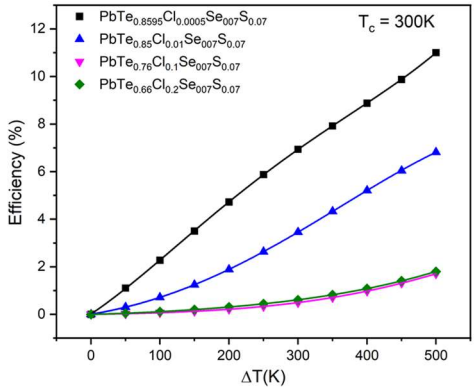

Fig.-4: Relationship between Efficiency (%) and the Temperature Gradient (ΔT) for $(PbTe_{0.93-x}Se_{0.07}Cl_x)_{0.93}PbS_{0.07}$ (x = 0.0005, 0.01, 0.1, and 0.2), Material Compositions at T_c = 300K.

Based on the experimental data illustrated in Fig.-5, $PbTe_{0.8595}Cl_{0.0005}Se_{0.07}S_{0.07}$ (black squares) records the highest Pd of approximately 5.2 W/cm^{-2} at ΔT = 500 K, resulting from superior $(PF)_{eng}$ values (0.85 $W/m\cdot K^2$ from Fig.-3). demonstrating that the ultra-low doping strategy achieves approximately 3.1 times higher power density performance for high-power-density thermoelectric applications.[18]

This study highlights the non-linear relationship between ΔT and performance indicators (ZT_{eng}, PF_{eng}, Pd), emphasizing the impact of material properties on efficiency.[20] Our findings demonstrate that optimized doping enhances performance at higher ΔT. $PbTe_{0.8595}Cl_{0.0005}Se_{0.07}S_{0.07}$ outperforms other compositions due to its optimal balance of electrical and thermal properties achieved through precise ultra-low chlorine doping control.[11] The significance of this work lies in identifying the critical doping threshold (x = 0.0005) that maximizes both efficiency (11%) and power density (5.2 W/cm^{-2}) simultaneously, representing a breakthrough in thermoelectric material optimization. The electronic contribution (κ_{el}) increases with increased doping, whereas the lattice contribution (κ_l) decreases due to phonon scattering. This highlights the complexity of thermal transport within thermoelectric materials.[9]

Optimal doping concentration enhances electrical conductivity by minimizing scattering effects, while maintaining a high Seebeck coefficient. The practical implications of these findings directly support global sustainability goals by enabling more efficient utilization of industrial waste heat, contributing to reduced energy waste, and supporting the transition to cleaner energy systems as outlined in SDG 7. However, excessive doping reduces performance due to increased scattering, which disrupts both electrical and thermal transport mechanisms critical for optimal thermoelectric function.

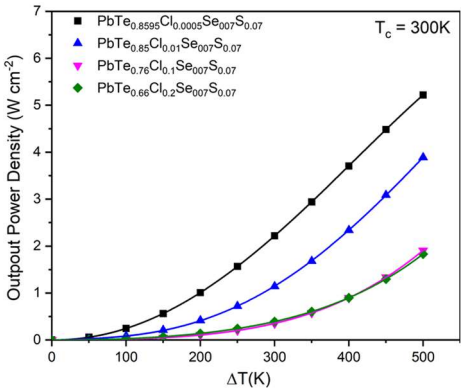

Fig.-5: Relationship between Output Power Density (*Pd*) and the Temperature Gradient (ΔT) for $(PbTe_{0.93-x}Se_{0.07}Cl_x)_{0.93}PbS_{0.07}$ (x = 0.0005, 0.01, 0.1, and 0.2) at T_c = 300 K

CONCLUSION

This research systematically investigated chlorine-doped $(PbTe_{0.93-x}Se_{0.07}Cl_x)_{0.93}PbS_{0.07}$ materials across varying doping concentrations (x = 0.0005-0.2) to optimize thermoelectric performance. Ultra-low chlorine doping (x = 0.0005) in $PbTe_{0.8595}Cl_{0.0005}Se_{0.07}S_{0.07}$ achieved exceptional performance through optimal electrical-thermal property balance, demonstrating a superior Seebeck coefficient (-237 $\mu V/K^{-1}$), power factor (21 $\mu W/cm^{-1}\cdot K^{-2}$), and minimal thermal conductivity (0.84 $W/m^{-1}\cdot K^{-1}$). Engineering evaluation revealed breakthrough achievements: ZT_{eng} of 0.69, PF_{eng} of 0.85 $W/m^{-1}\cdot K^{-1}$, 11% energy conversion efficiency, and 5.2 W/cm^{-2} power density at ΔT = 500 K. Ultra-low doping strategy achieved 6.8 times higher efficiency and 3.1 times higher power density compared to excessive doping, confirming precise doping control. These findings directly support SDG 7 (Affordable and Clean Energy) by enabling the conversion of industrial waste heat (20-50% of global energy losses) into usable electricity, advancing practical waste heat recovery systems. We recommend implementing ultra-low doping strategies ($x \leq$ 0.001), optimizing temperature gradients ($\Delta T \geq$ 400 K), and exploring scalability for industrial applications to advance sustainable thermoelectric technology deployment.

ACKNOWLEDGMENTS

The authors acknowledge the Mercubuana University, Jakarta, Indonesia.

CONFLICT OF INTEREST

The authors declare that there is no conflict of interest.

AUTHOR CONTRIBUTIONS

The present work is related to *SDG-7: Affordable and Clean Energy*. All the authors contributed significantly to this manuscript, participated in reviewing/editing and approved the final draft for publication. The research profile of the authors can be verified from their ORCID ids, given below:

Sukendar http://orchid.org/0009-0001-4279-5724
J.S. Rhee http://orchid.org/0000-0002-3656-2430
D. Ginting http://orchid.org/0000-0002-6538-7096

REFERENCES

1. A. M. Sargar, N. S. Patil, S. R. Mane, and P. N. Bhosale, *Rasayan Journal of Chemistry*, **2(2)**, 364(2009).
2. L.E. Bell, *Science*, **321(5895)**,1457(2008), https://doi.org/10.1126/science.1158899
3. J.P. Heremans, M.S. Dresselhaus, L.E. Bell, and D.T. Morelli, *Nature Nanotechnology*, **8(7)**, 471(2013), https://doi.org/10.1038/nnano.2013.129

4. T. Shiga, J. Shiomi, J. Ma, O. Delaire, T. Radzynski, A. Lusakowski, and G. Chen, *Physical Review B*, **85(15)**, Article No. 155203, (2012), https://doi.org/10.1103/physrevb.85.155203
5. J.P. Heremans, V. Jovovic, E.S. Toberer, A. Saramat, K. Kurosaki, A. Charoenphakdee, and G.J. Snyder, *Science*, **321(5888)**, 554(2008), https://doi.org/10.1126/science.1159725
6. I. Cohen, M. Kaller, G. Komisarchik, D. Fuks, and Y. Gelbstein, *Journal of Materials Chemistry C*, **3(37)**, 9559, (2015), https://doi.org/10.1039/c5tc01781e
7. G. Tan, F. Shi, S. Hao, L.-D. Zhao, H. Chi, X. Zhang, C. Uher, C. Wolverton, V.P. Dravid, and M.G. Kanatzidis, *Nature Communications*, **7**, Article No. 12167(2016), https://doi.org/10.1038/ncomms12167
8. C. Han, Z. Li, and S.X. Dou, *Chinese Science Bulletin*, **59(18)**, 2073(2014), https://doi.org/10.1007/s11434-014-0237-2
9. B. Fu, G. Tang, and Y. Li, *Physical Chemistry Chemical Physics*, **19(42)**, 28517(2017), https://doi.org/10.1039/c7cp04638c
10. L.D. Hicks and M.S. Dresselhaus, *Physical Review B*, **47(19)**,12727(1993), https://doi.org/10.1103/PhysRevB.47.12727
11. D. Ginting, C. Lin, J.H. Yun, B. Yu, S. Kim, and J. Rhyee, *Journal of Materials Chemistry A*, **5**, 2643, (2017), https://doi.org/10.1039/C7TA02643A
12. L.-D. Zhao, J. He, S. Hao, C.-I. Wu, T.P. Hogan, C. Wolverton, V.P. Dravid, and M.G. Kanatzidis, *Journal of the American Chemical Society*, **134(39)**, 16327(2012), https://doi.org/10.1021/ja306527n
13. J. He, M.G. Kanatzidis, and V.P. Dravid, *Materials Today*, **16(5)**,1369(2013), https://doi.org/10.1016/j.mattod.2013.05.004
14. Q. Zhang, B. Liao, Y. Lan, K. Lukas, W. Liu, K. Esfarjani, C. Opeil, D. Broido, G. Chen, and Z. Ren. *Proceedings of the National Academy of Sciences*, **110(33)**, 13261(2013), https://doi.org/10.1073/pnas.1305735110
15. W. Liu, H.S. Kim, Q. Jie, and Z. Ren, *Scripta Materialia*, **111**,3(2016), https://doi.org/10.1016/j.scriptamat.2015.07.045
16. S. A. Yamini, H. Wang, D. Ginting, D. R. G. Mitchell, S. X. Dou, and G. J. Snyder, *ACS Applied Materials & Interfaces*, **6(14)**, 11476(2014), https://doi.org/10.1021/am502140h
17. M. Sajid, I. Hassan, and A. Rahman, *Renewable and Sustainable Energy Reviews*, **78**, 15(2017), https://doi.org/10.1016/j.rser.2017.04.098
18. H.S. Kim, W. Liu, G. Chen, C.-W. Chu, and Z. Ren, *Proceedings of the National Academy of Sciences*, **112(27)**, 8205(2015), https://doi.org/10.1073/pnas.1510231112
19. W. Liu, J. Hu, S. Zhang, M. Deng, C.-G. Han, and Y. Liu, *Materials Today Physics*, **1**, 50(2017), https://doi.org/10.1016/j.mtphys.2017.06.001
20. N. Parse and S. Pinitsoontorn, *APL Materials*, **11(8)**, Article 081117(2023), https://doi.org/10.1063/5.0160055

[RJC-9282/2025]